Journal of Alloys and Compounds 378 (2004) 140–144

Journal of ALLOYS AND COMPOUNDS

www.elsevier.com/locate/jallcom

Acoustic characterization of the elastic properties of austenite phase and martensitic transformations in CuAlNi shape memory alloy

T. Černoch [a,*], M. Landa [b], V. Novák [a], P. Sedlák [b], P. Šittner [a]

[a] *Institute of Physics, Academy of Sciences of the Czech Republic, Na Slovance 2, 18221 Prague, Czech Republic*
[b] *Institute of Thermomechanics, Academy of Sciences of the Czech Republic, Dolejškova 5, 18200 Prague, Czech Republic*

Received 4 September 2003; accepted 14 October 2003

Abstract

A complete set of second and third order elastic constants of the cubic austenite phase in CuAlNi shape memory alloy was determined by ultrasonic pulse-echo method. Because of the very high elastic anisotropy of the austenite phase ($A = 12.02$), a negative Poisson ratio ν is obtained for loading the crystal in certain directions, e.g. $\nu_{12} = \nu_{21} = -0.62$ in the coordinate system [1 1 0], [1 $\bar{1}$ 0], [0 0 1]. Measurements of the third order elastic constants were carried out in nine selected specimen geometries (acoustic modes). The wave velocity was highly sensitive to the applied stress only in two shear modes. The onset of the stress-induced martensitic transformation (MT) was detected by acoustic emission (AE), ultrasonic wave velocity and attenuation measurements in given order. The acoustic emission was thus the most sensitive acoustic method for detection of early stages of the transformation.

Keywords: Intermetallics; Anisotropy; Elasticity; Ultrasonics

1. Introduction

Shape memory alloys (SMA) are intermetallic ordered alloys (Cu–Al–Ni, Cu–Zn–Al, Ni–Ti, Ni–Mn–Ga, etc.), often strongly elastically anisotropic. When the stress-induced martensitic transformation (MT) proceeds in a SMA single crystal, it transforms into a metastable two phase composite consisting of plate-like particles of the martensite phase within the parent austenite phase. The phases are separated by highly mobile phase interfaces and have different elastic constants. Knowledge of the constants describing the linear elastic behavior (second order elastic constants, SOEC) of both phases in SMAs is essential to describe reliably the mechanical behaviors of SMAs.

The nonlinear elasticity of solids can be described in first approximation using third order elastic constants (TOEC). The macroscopic nonlinear elasticity is associated with lattice vibrations anharmonicity and with asymmetry of the atomic binding energy well [1]. Therefore, investigation of the TOECs is a key to understanding of the lattice stability of SMAs [2]. A complete set of TOECs of the cubic austenite phase of Cu-based SMAs single crystals near and far above the transformation temperature was reported earlier by Gonzales-Comas and Manosa [2] who applied only very small compression stresses of the order of 10 MPa to the cube specimens. In the present work, similar alloy and the same cube sample geometry is used. The aim of this work was to check their results and extend the measurements of the wave propagation towards larger applied stresses in austenitic state as well as investigate additional acoustic properties (ultrasonic attenuation and acoustic emission, AE) in situ during the stress-induced martensitic transformation.

2. Experimental

2.1. The specimen

Oriented single crystals of Cu–14.3Al–4.1Ni (wt.%) alloy were grown by seeded Bridgman technique. The specimens were heat treated by annealing at 900 °C for 2 h in argon atmosphere and quenched in ice water to bring the specimens into $L2_1$ (β-phase) ordered austenite crystal structure at room temperature with transformation

* Corresponding author. Tel.: +420-266-052-778; fax: +420-286-890-527.
E-mail address: cernoch@fzu.cz (T. Černoch).

0925-8388/$ – see front matter © 2004 Elsevier B.V. All rights reserved.
doi:10.1016/j.jallcom.2003.10.093

Table 1
Measured velocities of acoustic waves in austenite

Directions	c_0 measured (mode type)			
	L	T	qL	qT_a
[N]-propagation	[0 0 1]	[0 0 1]	[1 1 0]	[1 1 0]
[U]-polarization	[0 0 1]	(0 0 1)	[1 1 0]	[1 $\bar{1}$ 0]
c_0 [N][U] (mm/μs)	4.50	3.69	5.72	1.06
Std (c_0) (mm/μs)	—	0.006	0.001	0.004

Table 2
Orientation of cubes for TOEC measurement.

Mode number	Mode type	[M]-loading	[N]-propagation	[U]-polarization
(1)	qL	[0 0 1]	[1 1 0]	[1 1 0]
(2)	qT_a	[0 0 1]	[1 1 0]	[1 $\bar{1}$ 0]
(3)	qT_b	[0 0 1]	[1 1 0]	[0 0 1]
(4)	L	[1 $\bar{1}$ 0]	[0 0 1]	[0 0 1]
(5)	T	[1 $\bar{1}$ 0]	[0 0 1]	[1 $\bar{1}$ 0]
(6)	T	[1 $\bar{1}$ 0]	[0 0 1]	[1 1 0]
(7)	qL	[1 $\bar{1}$ 0]	[1 1 0]	[1 1 0]
(8)	qT_a	[1 $\bar{1}$ 0]	[1 1 0]	[1 $\bar{1}$ 0]
(9)	qT_b	[1 $\bar{1}$ 0]	[1 1 0]	[0 0 1]

temperatures $M_s(\gamma_1') = 193\,K$, $A_f(\gamma_1') = 228\,K$. Cube specimens 10 mm × 10 mm × 10 mm for compression tests were spark cut with the faces parallel to the $(1\,1\,0)_A$, $(-1\,1\,0)_A$ and $(0\,0\,1)_A$ planes.

2.2. SOEC and TOEC measurement and calculation

We have measured all independent SOEC and TOEC of austenite. There are only three independent SOEC ($\underline{C}_{11}$, $\underline{C}_{12}$, $\underline{C}_{44}$) and six independent TOEC ($\underline{C}_{111}$, $\underline{C}_{112}$, $\underline{C}_{123}$, $\underline{C}_{144}$, $\underline{C}_{166}$, $\underline{C}_{456}$) for cubic crystals [11]. Both SOEC and TOEC were evaluated from ultrasonic wave velocity and density measurements determined by the Archimedes technique. The standard pulse-echo method [3] was used for measurement of the velocity of longitudinal (L, qL) and transverse (T, qT_a) acoustic waves propagating in the crystal directions listed in Table 1. Elastic constants C_{11}, C_{12} and C_{44} were evaluated from the wave velocities [10]. The wave velocities during loading were related to the actual and original specimen dimension in the direction of wave propagation H_0 and denoted v and v_0, respectively, c_0 stands for the wave velocity in the stress-free specimen and ρ_0 is the density.

The TOECs can be evaluated from the known SOECs and measurements of the wave velocities in nine directional configurations of the single crystal (Table 2) under uniaxial compression using Thurston–Brugger's equation [5]. Initial slope of the stress dependence of the ultrasonic wave velocity is used. The maximal reached compression stress of 200 MPa was still much lower than the stresses triggering the onset of the stress-induced MT (400 MPa (modes 1–3) and 800 MPa (modes 4–9)). All measurements were carried out at room temperature $T = 297\,K$.

2.3. Further acoustic measurements

An immersion two-channel pulser/receiver ultrasonic system was employed for a more detailed study of hysteresis of longitudinal waves velocity. It was motivated by the facts that: (i) the immersion system is non-contact (surface deformation of the sample otherwise influences acoustic coupling of the direct contact transducers), and (ii) enables simultaneous measurement of the specimen thickness and the related time of flight allowing more precise evaluation of the wave velocity in the deforming specimen [6]. This somewhat unusual configuration is described in detail in [8]. Martensitic transformations in SMAs are accompanied by an intensive acoustic emission, which can be beneficially utilized for detection and kinetic characterization of the transformation processes. The AE was monitored during the test focussing on the identification of the start of the MT (for details, see [7]).

3. Results and discussion

3.1. Elastic constants

The wave velocities measured by the standard pulse-echo method in the stress-free specimen are summarized in Table 1. The determined values of SOECs (Table 3) indicate, that the Cu–Al–Ni austenite phase has a very high anisotropy (anisotropy factor $A = 12.02$). In certain geometry, e.g for loading along x-axis in a coordinate system [1 1 0], [1 $\bar{1}$ 0], [0 0 1] even negative Poisson ratio $\nu_{12} = \nu_{21} = -0.62$ is obtained. Negative Poisson ratio has also been reported for 2H martensite phase in the Cu–Al–Ni alloy [9] indicating that the large anisotropy is inherited (though in lower extent) by the product martensite phase.

Relative change of velocities upon loading, measured by the standard pulse-echo method is depicted in Fig. 1. Definition of modes is in Table 2 while the fitted TOECs are listed in Table 3. The TOEC's values differ up to about 50% from the values reported by Gonzales-Comas and Manosa [2] for a similar alloy ($A = 13.1$) at temperature $T = 293K$.

Table 3
Second and third order elastic constants of austenite

	C_{11} (Gpa)	C_{12} (GPa)	C_{44} (GPa)	A (1)	C_{111} (TPa)	C_{112} (TPa)	C_{123} (TPa)	C_{144} (TPa)	C_{166} (TPa)	C_{456} (TPa)
Value	142.80	126.84	95.90	12.02	−1.65	−0.62	−0.48	−0.60	−0.69	−0.56
S.D.		0.15	0.30		0.17	0.13	0.08	0.08	0.01	0.06

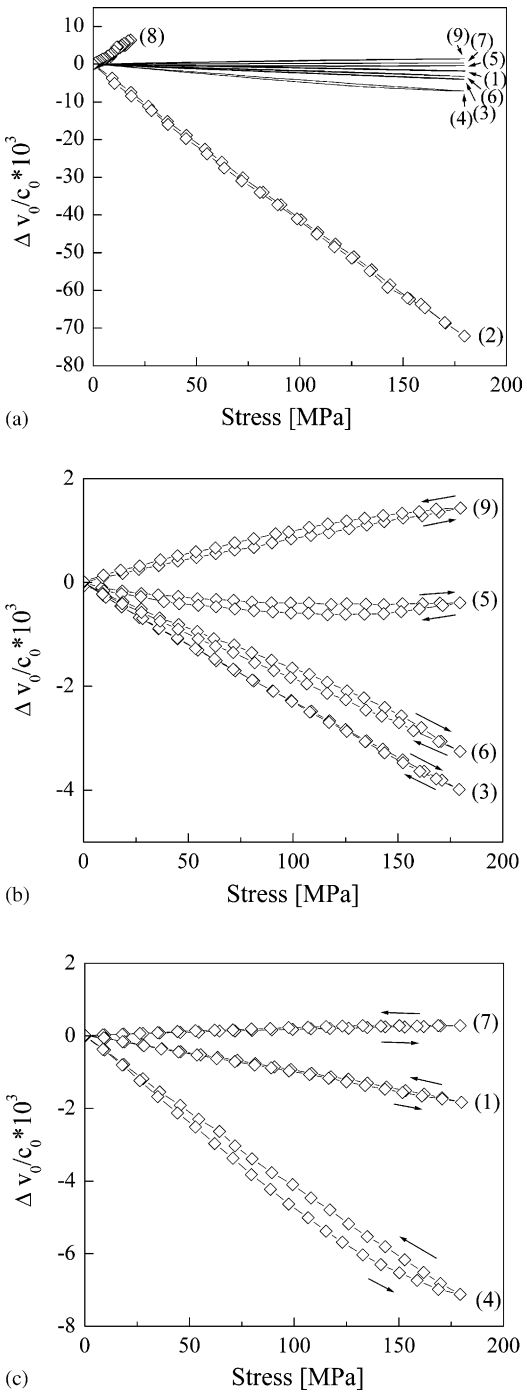

Fig. 1. Relative changes of natural wave velocity during loading in compression measured by pulse-echo ultrasonic technique in (a) all modes (curves with marks belong to qT_a modes), (b) qT_b and (c) L, qL modes.

Nevertheless, the measured values of TOECs fulfil the conditions $C_{ijk} < 0$ and $C_{111} < C_{112} < C_{123}$ arising from the atomic binding force relation [4]. The qT_a-modes numbers (8 and 2) are the most sensitive ones to the applied stress (Fig. 1a). This can be ascribed to the intrinsic shear instability associated with the martensitic transformation, which is being approached upon stressing. The longitudinal wave mode number (4) is the next most sensitive one. This

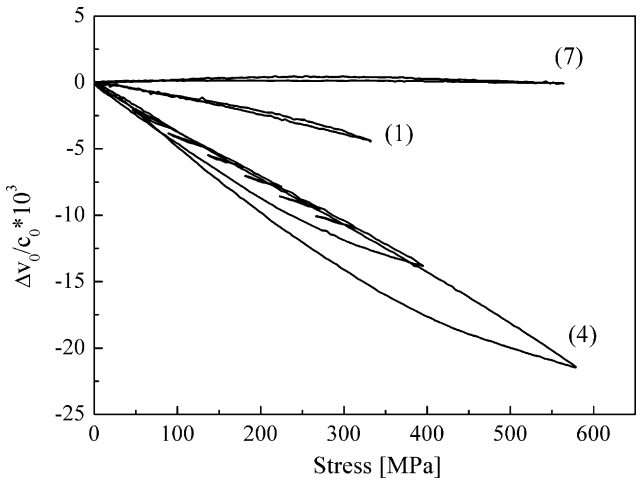

Fig. 2. Relative changes of natural wave velocity in L and qL modes during loading in compression using immersion technique. The partial unloads in mode number (4) indicate that the unusual hysteresis occurs also at very low stresses.

mode shows (Fig. 1c) an unusual hysteresis in dependence of stress. However, the transverse wave modes numbers (6, 5 and 9) also show a similar hysteresis although less pronounced. It thus seems that the hysteresis is more related to the load axis orientation (the hysteresis was observed for loading along ⟨0 1 1⟩ direction) than to the type of ultrasonic wave.

In order to exclude possible experimental artefacts leading to the hysteresis, modes L and qL were measured also by the immersion technique (Fig. 2). Taking advantage of the simultaneously measured transverse strain, the changes of instantaneous velocity $\Delta v/c_0$ may be corrected for the dimensional changes taking place due to the transverse deformation. The peculiar mode number (4) with hysteresis was measured with partial unloads (Fig. 2) during the test starting from very small stresses. Since the hysteresis was clearly observed even for the smallest stresses, the phenomenon shall not be related directly to the MT. No plausible explanation is available yet, but a dissipative mechanism based on a presence of non-stochiometric vacancies allowing for short range elastic dipole reorientation processes in stressed austenite with very fast kinetics is a potential candidate. Similar mechanisms has been considered by Pelegrina and Ahlers [11] or Otsuka and Ren [12] to explain stabilization phenomena in stressed austenite and martensite phases, respectively.

3.2. Start of the MT

The martensitic transformations in SMA's are accompanied by intensive acoustic emission, which can be beneficially utilized for detection and kinetic characterization of the transformation processes [7]. The AE activity measured during stress-induced martensitic transformation in compression test is plotted in dependence on strain in Fig. 3a.

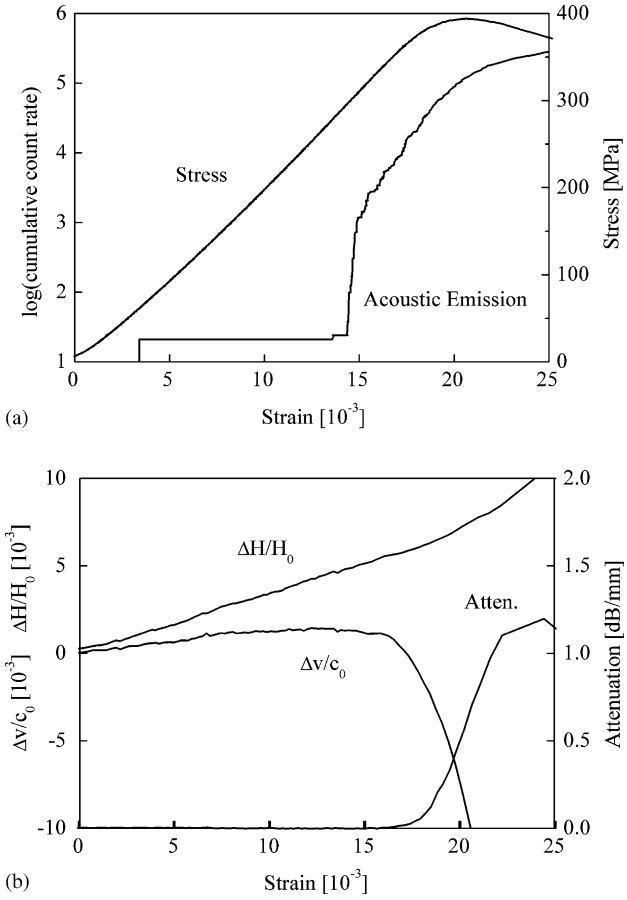

Fig. 3. Identification of the start of the martensitic transformation in mode number (1) by different methods. Changes of (a) stress and acoustic emission cumulative count rate and (b) relative change of natural velocity, specimen transverse dimension and attenuation of the amplitude of longitudinal wave during the compression straining.

The start of the austenite to martensite transformation is clearly identified as a sudden increase of the cumulative AE count rate occurring in the elastic range much earlier before any nonlinearity on the stress–strain curve is detected.

The relative changes of other measured quantities—wave velocity $\Delta v/c_0$, transverse strain $\Delta H/H_0$ and attenuation—are plotted in dependence on the compression stress in Fig. 3b. Each of the five mentioned quantities can be used to detect the start of the transformation process. The evaluated threshold strains (stresses), however, significantly differ. The AE signal starts to grow first (at $\sigma = 300$ MPa), than the wave speed and attenuation start to change due to the sufficient number of already triggered transformation events (although still in the apparently elastic range) and, finally, the transverse strain and macroscopic stress evidence the onset of the macroscopic transformation process. The reason for these differences comes from the fact that various signals are sensitive to different changes in material state associated with MT. While the acoustic emission is generated by local and dynamic changes, the wave speed and attenuation characterize average quantity over the specimen volume, the macroscopic stress and transverse strain are related to the volume fraction of the transformed phase.

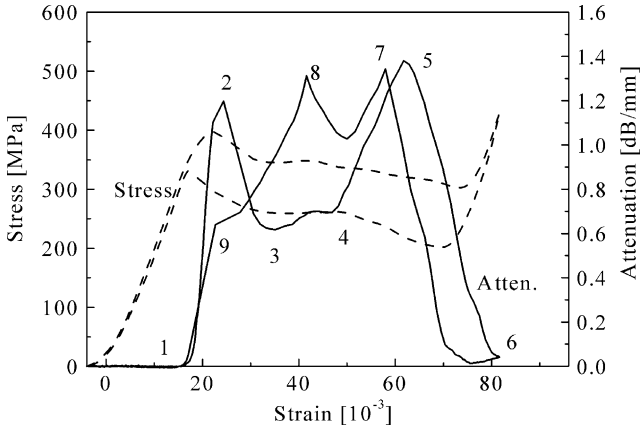

Fig. 4. Development of the attenuation of amplitude of longitudinal wave along the pseudoelastic stress–strain curve in compression (mode number (1)).

3.3. Course of the MT

Finally, ultrasound attenuation during the stress-induced transformation was measured using the longitudinal wave (Fig. 4). It follows from simultaneous optical observations of the specimen surface that forward MT starts by formation of thin bands of β_1' martensite. The sudden stress drop corresponds to the formation of relatively big particle of the γ_1' martensite and further deformation is due to motion of the macroscopic β_1/γ_1' interface. At maximum stresses, the γ_1' (2*H*) martensite was nearly single crystal with only a few twinning interfaces inside, as indicated by the very low value of attenuation (point 6 in Fig. 4). The reverse transformation back to the austenite seems to proceed in a different way—a complex microstructure suggesting twinning in martensite bands appears first and a mixture of austenite and twinned martensite bands is dominant near the end of the reverse transition. The evolution of the attenuation corresponds well to this optical observations, indicating different processes and structures in forward and reverse transitions.

4. Conclusions

Elastic properties and martensitic transformations in single crystals of Cu–Al–Ni shape memory alloys were investigated by acoustic methods. Complete set of second and third order elastic constants of cubic austenite phase was determined. Five different quantities—acoustic emission, ultrasonic attenuation and wave velocity, transverse strain and macroscopic stress were measured during the stress-induced martensitic transformation. The threshold strains (stresses), evaluated using each quantity increases in given order since various signals are sensitive to different changes

in material state associated with MT. The development of ultrasonic attenuation during forward and reverse stress-induced martensitic transformation indicates (in agreement with optical observation) that different transformation processes take place during the transition from austenite to γ_1' martensite and from γ_1' martensite to austenite.

Acknowledgements

Supports of the Grant Agency of the ASCR (contract no. A1048107) and Grant Agency of the Czech Republic (contracts 106/01/0396 and 106/00/D106) are sincerely acknowledged.

References

[1] M.A.Breazeale, J. Philip, Determination of third-order elastic constants from ultrasonic harmonic generation measurements, in: W.P. Mason, R.N. Thurtson (Eds.), Physical Acoustics, vol. XVII, Academic Press, London, UK, 1984, pp. 2–61.
[2] A. Gonzales-Comas, Ll. Manosa, Philos. Mag. A 80 (2000) 1681–1697.
[3] E.P Papadakis, T.P. Lerch , Pulse superposition, pulse-echo overlap and related techniques, in: M. Levy, H.E. Bass, R.R. Stern (Eds.), Handbook of Elastic Properties of Solids, Liquids and Gases, vol. I–IV, Academic Press, 2001.
[4] D.Y. Li, X.F. Wu, T. Ko, Philos. Mag. A 63 (1991) 585–601.
[5] R.N. Thurston, K. Brugger, Phys. Rev. 133 (1964) A1604–A1610.
[6] D.K. Hsu, M.S. Hughes, J. Acoust. Soc. Am. 92 (Part 1) (1992) 669–675.
[7] M. Landa, V. Novák, M. Blaháček, P. Šittner, J. Acoust. Emission 20 (2002) 163–171.
[8] M. Landa, V. Novák, P. Sedlák, P. Šittner, in: W. Sachse (Ed.), Ultrasonic characterization of Cu–Al–Ni single crystals lattice stability in the vicinity of the phase transition, Ultrasonics, Special Issue of the Conference Ultrasonic International 2003, Granada, Spain, 2003 (accepted).
[9] M. Rovati, Scripta Mater. 48 (2003) 235.
[10] J.F. Nye, Physical Properties of Crystals, Oxford University Press, 1985.
[11] J. Pelegrina, M. Ahlers, Scripta Mater. 50 (2004) 423–427.
[12] K. Otsuka, X. Ren, Scripta Mater. 50 (2004) 207.